Structure solution of the $Al_{69.2}Cu_{20}Cr_{10.8}$ ϕ-phase

Shmuel Samuha[a], Rimon Tamari[b], Benjamin Grushko[c], Louisa Meshi[b*]

[a] *NRCN, P.O. Box 9001, Beer-Sheva 84190, Israel*

[b] *Department of Materials Engineering, Ben Gurion University of the Negev, Beer Sheva 84105, Israel*

[c] *Peter Grünberg Institut, Forschungszentrum Jülich, Jülich 52425, Germany*

**Corresponding author: louisa@bgu.ac.il*

Synopsis - type the synopsis here (Style: IUCr synopsis)

Abstract

The stable ϕ-phase forming below ~650 °C around the $Al_{69.2}Cu_{20.0}Cr_{10.8}$ composition was found to be hexagonal ($P6_3$, a = 1.1045(2), c = 1.2688(2) nm) and isostructural to the earlier reported $Al_{6.2}Cu_2Re$ X-phase [Samuha *et al*, (2016)]. Using the structural model of the latter, a successful Rietveld refinement of the XRD data for $Al_{69.5}Cu_{20.0}Cr_{10.5}$ was performed. Both ϕ and X were found to be structurally related to the $Al_{72.6}Cu_{11.0}Cr_{16.4}$ ζ-phase ($P6_3/m$, a = 1.7714, c = 1.2591 nm [Sugiyama *et al.*, (2002)], with a close lattice parameter c and a τ-times larger lattice parameter a (τ is the golden mean). The structural relationship between ζ and ϕ was established based on the similarity of their layered structures and the common construction features. Additionally, the strong-reflection approach was successfully applied for the modeling of the ϕ-phase based on the structural model of the ζ-phase. The simulated and experimental structural models were found to be essentially identical.

Keywords: intermetallics; Rietveld refinement; strong-reflections approach, electron crystallography; structure prediction; crystal structure

1. Introduction

Investigation of the Al–Cu–Cr alloy system revealed a number of stable intermetallics, structures of which were only partially characterized (Grushko, 2017 and references therein). In the temperature range of 570-800 °C and compositional range above 40 at.% Al, apart from the binaries, eight additional ternary compounds designated as ζ, κ, ψ, S, ϕ, σ, β and Λ were revealed. The structures of the ζ-phase of $Al_{72.6}Cu_{11.0}Cr_{16.4}$ and the κ-phases of $Al_{67.4}Cu_{14.3}Cr_{18.3}$ were determined by single-crystal X-ray diffraction [Sugiyama *et al.*, 2002] [1].

In the present work we report the results of the structure solution of the ϕ-phase and its structural relationship to the ζ-phase. The ϕ-phase was found to be formed at 650 °C in a small compositional

[1] In (Sugiyama *et al.*, 2002) the latter is designated β.

region around ~$Al_{70}Cu_{19}Cr_{11}$, while already at 700 °C the same composition has been associated with the S-phase, whose compositional region was found to extend towards ~$Al_{79}Cu_{10}Cr_{11}$.

The structure solution of the ϕ-phase was performed by Rietveld refinement of the XRD data based on the structural model of the isostructural $Al_{6.2}Cu_2Re$ X-phase [Samuha *et al*., 2016]. Additionally, a structural model of the ϕ-phase was deduced from the known structure of the ζ-phase using the strong-reflections approach. Both models were proved to be essentially identical.

2. Experimental

An $Al_{69.5}Cu_{20.0}Cr_{10.5}$ alloy was produced from the constituent elements by levitation induction melting in a water-cooled copper crucible under an Ar atmosphere. The purity of Al was 99.999%, of Cu 99.95% and of Cr 99.99%. The sample was annealed under vacuum for 424 h at 650 °C.

The alloy was studied by scanning electron microscopy (SEM), powder X-ray diffraction (XRD) and transmission electron microscopy (TEM). The compositions were analyzed by energy-dispersive X-ray analysis (EDX) in SEM. For the XRD examinations, the material was powdered in an agate mortar. The XRD pattern was recorded on a Rigaku D/MAX-2000 diffractometer equipped with a graphite monochromator for the Cu Kα radiation. The measurements were performed within the 2θ range from 5 to 100° with the step size of 0.02° and the counting rate of 10 s/step. The FULLPROF software [Rodrigues, 1998] was used for the analysis of the XRD data.

For the TEM examinations, the powdered material was dispersed on a grid with a carbon film. The TEM study was carried out on a FASTEM JEOL-2010 electron microscope equipped with the Nanomegas "Spinning Star" precession unit. Diffraction patterns with a 120 mm camera length were recorded on a top-mounted Gatan Model 780 Dual Vision 300 camera with 1030x1300 pixels. The simulations of the Precession Electron Diffraction (PED) patterns were performed using the program eMAP [Oleynikov, 2011]. This program also allowed obtaining the theoretical structure factors, calculating the three-dimensional Electron-Density Maps (EDM) and extracting atomic positions from EDMs.

3. Results and discussion

3.1. Refinement of the ϕ-phase structure

The SEM examinations of the $Al_{69.5}Cu_{20.0}Cr_{10.5}$ alloy annealed at 650 °C revealed a two-phase structure: the major phase with the composition close to that of the alloy and a minor phase of ~$Al_{45.4}Cu_{53.7}Cr_{0.9}$. Since the corresponding complex powder XRD pattern could not be indexed using only known phases in this ternary system, the material was examined by electron diffraction in TEM. The corresponding PED patterns of the major ϕ-phase indicated a hexagonal structure with the lattice parameters a = 1.10 and c = 1.275 nm.

The crystal system, unit cell parameters and intensity distribution in the PED patterns of the ϕ-phase were found to resemble those of the Al–Cu–Re X-phase ($P6_3$, a = 1.1029 and c = 1.2746 nm, Meshi *et al*. 2009). For example, the PED patterns along [100] of the ϕ-phase and X-phase are compared in Figs. 1a and 1b, respectively. The crystal structure of the Al–Cu–Re X-phase was deduced by Samuha *et al*. (2016) through the application of *Direct Methods* on the PED Tomography (PEDT) data and refined against the powder XRD data by the Rietveld method.

These results allowed successful indexing of the major phase in the above-mentioned powder XRD pattern. The additional reflections of the minor phase were associated with those of the Al–Cu orthorhombic phase ζ_{1Cu} (Al_3Cu_4, *Fmm*2, $a \approx 0.814$, b ≈ 1.43, $c \approx 1.0$ nm, Gulay *et al*., 2004)[2].

The ϕ-phase and X-phase are formed around quite close equivalent compositions $Al_{69.5}Cu_{20.0}Cr_{10.5}$ and $Al_{65}Cu_{25}Re_{10}$ in the Al-Cu-Cr and Al-Cu-Re phase diagrams, respectively while $Al_{6.2}Cu_2Re$ ($Al_{67.4}Cu_{21.7}Cr_{10.9}$) composition (which can be determined from the model proposed in Samuha *et al* (2016)) is in between these two compositions. The deviation of the model composition from the measurements was ignored in [Samuha *et al*., 2016]. Considering the close atomic percentage of Cr and Re in these phases, the corresponding atoms could occupy the same cites, while some Cu in X phase could be replaced by Al in ϕ phase.

The correctness of this assumption was confirmed by the comparison of the experimental and simulated PED patterns of the ϕ-phase in Figs. 1a and 1c, respectively. The latter was calculated from the structural model of the Al–Cu–Re X-phase, where Re was replaced by Cr, while Al and Cu were still fixed at their original positions. Indeed, Figs. 1a and 1c illustrate similar positions of the reflections (i.e. prove the correctness of the geometry of the unit cell) and the fact that the strongest reflections in both patterns are distributed in a similar manner and hierarchy points on the correctness of the proposed atomic model.

Therefore, the model of the X-phase was used as a starting point for the deduction of the structural model of the ϕ-phase. It was refined by the Rietveld method on the powder XRD pattern using the FULLPROF software [Rodrigues, 1998]. For convenience, the major ϕ-phase was refined in the Rietveld mode, while the minor ζ_{1Cu}-phase was refined applying the profile matching mode (i.e. refining only the geometry, without taking atom positions into account).

In order to adjust the compositions, one could suggest that a 2-fold Cu site and a 2-fold Al site in the model published in Samuha *et al*. (2016) would be occupied by either both Cu or both Al, which would result in $Al_{64}Cu_{18}Cr_{10}$ = $Al_{69.6}Cu_{19.5}Cr_{10.9}$ and $Al_{60}Cu_{22}Cr_{10}$ = $Al_{65.2}Cu_{23.9}Re_{10.9}$. This was not confirmed by the refinement of the ϕ-phase, which exhibited better results suggesting partial occupancy.

[2] The composition of the minor phase is almost binary. There are three phases in the relevant compositional region of Al–Cu. Although at the annealing temperature of 650 °C the ε_{2Cu}-phase would be expected in equilibrium with ϕ, this was not confirmed by powder XRD. The binary ζ_{1Cu}–phase is formed in a lower temperature range in solid state, but it could be stabilized by the addition of Cr. Alternatively it could transform from ε_{2Cu} during cooling.

Thus, two out of four Cu 6-fold sites were suggested to be partially occupied by Al due to their position in the Cr coordination icosahedron. The details of the Rietveld refinement are summarized in Table 1, the atomic positions and thermal displacement factors are presented in Table 2.

The agreement factors for the refinement were: R_p = 2.66%, R_{wp} = 3.49%, R_{Bragg} = 6.66% (of the ϕ-phase) , R_{Bragg} = 0.788% (of Al_3Cu_4). The calculated and observed XRD profiles and the difference between them, as obtained following the refinement, are shown in Fig. 2. The interatomic distances are listed in Table 3. The occupancy refinement process led to the realistic stoichiometry of $Al_{69.2}Cu_{20.0}Cr_{10.8}$ and exhibited convergence.

The difference in the equivalent compositions of the ϕ-phase and X-phase illustrates importance of the electron concentration for the stability of these phases. Indeed, in order to compensate the increase of the absorption of 10 electrons by ~10 Re atoms replaced by Cr, ~5 atoms of Cu (each contributing only one electron) should be replaced by Al (each contributing three electrons). Therefore, in order to keep the same atomic structure - ϕ-phase in the Al-Cu-Cr system had to form with different (as compared to X phase) stoichiometry. These effects in resulting stable atomic structures of allumindes were thoroughly discussed in [Uziel *et al*., 2015, Yaniv *et al*., 2018, Yaniv *et al*., 2020]. At the composition equivalent to that of the Al–Cu–Re X-phase the so-called ψ-phase is formed in Al–Cu–Cr and has different atomic structure [Grushko, 2017].

An analysis of the simulated PED patterns of ϕ and ζ revealed similar intensity distributions of the corresponding reflections (see Fig. 3). For convenience, the positions of the exceptionally strong reflections in these patterns are emphasized using blue, green and red circles, each equal for both in the same orientation. As can be seen, the strong reflections are distributed in a similar manner along these circles in both patterns. These structures are characterized by the related space groups $P6_3$ and $P6_3/m$, respectively, and have essentially the same *c* lattice parameters, while their *a* lattice parameters 1.10 and 1.76 nm are approximately related by τ (where $\tau = (1 + \sqrt{5})/2 \approx 1.618$ is the golden mean). Their structural relation is quantitatively verified below using the strong-reflections approach [Christensen, 2004, Christensen *et al*., 2004].

3.2. Modeling of ϕ from the structure of ζ using the strong-reflections approach

The modeling is based on the extraction of the atomic positions of a *target* structure from a three-dimensional Electron Density Map (EDM) calculated by the inverse Fourier transform of the structure-factors amplitudes and adopted phases of the strong reflections of a *related source* structure.

For the deduction of the structure of ϕ, the reflections of ζ were *hand-picked* based on the compatibility of the distribution of the strong reflections present in the PED patterns of the two structures. As mentioned above, the only geometrical difference between ζ and ϕ is in the length of their lattice parameters *a*, meaning that for the structure comparison only translation element is needed. Thus,

the orientation matrix (A) was constructed for the re-indexation of the strongest reflections, following Equation 1. As can be seen, using Equation 1, a new set of the h, k indexes of ϕ was obtained simply by re-indexing the h, k indexes of ζ ($a_\phi/a_\zeta \approx 1.1/\ 1.7714 \approx 1/\tau$).

Equation 1
$$(hkl)_\phi = \begin{pmatrix} 1/\tau & 0 & 0 \\ 0 & 1/\tau & 0 \\ 0 & 0 & 1 \end{pmatrix} (hkl)_\zeta$$

It should be mentioned that this procedure was only carried out for the strongest reflections of ζ which were found to be compatible (comparing the net and ideal symmetry) to those of ϕ. After the re-indexation, the strongest reflections in the PED patterns of ϕ exhibited one-to-one correspondence to those of ζ, (see Fig. 3). For example the strongest reflections $(710)_\zeta \xrightarrow{(1)} (410)_\phi$ and $(063)_\zeta \xrightarrow{(1)} (043)_\phi$.

Next, the structure factors phases, which mainly determine the atomic positions in a structure, were modified based on their symmetry. For the structurally related compounds, the relations of the structure factor phases of the strongest reflections are close [Christensen, 2004, Christensen *et al*., 2004], which is the case for ζ and ϕ indeed. Due to the difference in the existence or lack of the center of symmetry, the structure factor phases of the strongest reflections of ζ should be modified by a shift of the origin, compatible with the space group of ϕ, which is non-centrosymmetric. For this case, from comparing common clusters (which will be presented in the next section), a shift of the origin was found to be (-0.34, 0.40, -0.02). The new structure factor phases were calculated using Equation 2:

Equation 2
$$\varphi'(hkl) = \varphi'(hkl) + 360° \cdot (h \cdot -0.34 + l \cdot 0.4 + k \cdot -0.02)$$

Following the shift of the origin, the phases of the symmetrically related reflections were close to those required by the symmetry of ϕ. Using the eMAP software [Oleynikov, 2011], 3D-EDMs were calculated by the inverse Fourier transform of the structure factors. The calculation was based on the re-indexed strongest reflections of ζ incorporating the corresponding structure factors amplitudes and modified phases. The resulting 3D-EDM viewed along the [001] orientation is shown in Fig. 4a. Following the 'peak hunting' procedure in eMAP [Oleynikov, 2011], the full theoretical model of ϕ was received. Thus, using a limited number of strong reflections, a successful deduction of the structure model of ϕ, based on that of ζ, was obtained. Comparing the experimental structure of ϕ (Fig. 4b) to that deduced from ζ a close similarity is seen. Using the Compstru software [Tasci *et al*., 2012], a quantitative comparison of the atomic models, i.e. model listed in Table 2 (determined using Rietveld refinement) with those derived applying strong reflections approach, the measure of similarity [Bergerhoff *et al*., 1999] was found to be Δ = 0.04 with the largest interatomic distance d = 0.56 Å, meaning essential identity.

3.3. Family of τ-related hexagonal structures in Al-based alloy systems

While the ϕ-type structure was only revealed in the Al–Cu–Cr(or Re) alloy systems, the ζ-type structure is also known in the Al–Cr–Ni [Grushko *et al*., 2008], Al–Cr–Pd [Kowalski *et al*., 2010] and in Al–Mn–Co(or Ni, or Fe) [Grushko *et al*., 2016]. In addition to this family, there is an hexagonal λ-Al_4Mn structure ($P6_3$/m, a = 2.8382, c = 1.24 nm, Kreiner & Franzen, 1997) with the lattice parameter c close to those of ϕ and ζ and the lattice parameter a about τ-times larger than that of ζ. All this points at large family of related phases.

Both ϕ and ζ can be presented as a six-layered structure perpendicular to the c-axis (see Fig. 5). The common description of their layers includes the type and packing: there are two approximately flat layers (designated as F and f) and four puckered thick layers (designated as P, P', p, p'). The layers are organized in the PFP'pfp' sequence where the PFP' layers are related by the 2_1 screw axis to the pfp' layers. In the ϕ-structure, the puckered layers consist of atoms that are arranged in such a way, as if a pseudo-mirror exists in each of the flat layers. The only difference between the ϕ and the ζ structures, in this respect, is that the later can be regarded as a mirror rather than a pseudo-mirror, as a result of the higher symmetry of ζ ($P6_3/m$ vs. $P6_3$).

This atoms in ϕ have similar icosahedral coordination. The I3-cluster [Kreiner *et* al., 1997, Mo *et* al., 2000] is of particular interest. It is constructed from three icosahedra built around the Cr atoms positioned in the flat layers. Since this cluster is not only present, but also distributed in a similar manner in both structures, it can be regarded as the fundamental structural unit. The position of this cluster (presented in Fig. 6), in both structures is identical if a shift of the origin to (-0.34, 0.40, -0.02) is introduced. These facts provide proofs from the real space for the correctness of atomic model and structural relationship, as there are many structural similarities between the structures of ϕ and ζ, mainly in their fundamental building blocks and layers.

4. Conclusions

The Rietveld refinement of the powder XRD data for the $Al_{69.5}Cu_{20.0}Cr_{10.5}$ ϕ-phase ($P6_3$, a = 1.1045(2), c = 1.2688(2) nm) was successfully performed on the basis of the structural model of the isostructural $Al_{6.2}Cu_2Re$ X-phase. Using the strong-reflections approach these phases were found to be structurally related to the $Al_{72.6}Cu_{11.0}Cr_{16.4}$ ζ-phase ($P6_3/m$, a = 1.7714, c = 1.2591 nm) with a close lattice parameter c and a τ-times larger lattice parameters a (τ is the golden mean). Structural similarities between the ζ-phase and ϕ-phase imply their attribution to the same family of the τ-related phases.

Acknowledgements- The authors thank C. Thomas for alloy preparation.

References

- Bergerhoff, G., Berndt, M., Brandenburg, K., Degen, T. (1999). Acta Cryst. B. 55, 147-156.

- Christensen, J. (2004). Licentiate Thesis, Department of Structural Chemistry Arrhenius Laboratory, Stockholm university, Stockholm, Sweden.
- Christensen, J., Oleynikov, P., Hovmöller & S., Zou, X.D. (2004). Ferroelectrics. 305, p.273–277.
- Grushko, B. (2017). J. Alloys Comp. 729, 426-437
- Grushko, B., Kowalski, W., Przepiórzyński, B., Pavlyuchkov, D. & Surowiec, M. (2008). J. Alloys Comp. 460, 299-304.
- Grushko, B., Pavlyuchkov, D., Mi, S. & Balanetskyy, S. (2016). J. Alloys Comp. 677, 148-162.
- Gulay, L. D., & Harbrecht, B. (2004). J. Alloys Comp, 367(1-2), 103-108.
- Kowalski, W., Grushko, B., Pavlyuchkov, D. & Surowiec, M. (2010). J. Alloys Comp. 496, 129-134.
- Kreiner, G., & Franzen, H. F. (1997). J. Alloys Comp, 261(1-2), 83-104.
- Meshi, L., Grushko, B., & Ezersky, V. (2009). J. Alloys Comp, 488(1), 108-111.
- Mo, Z. M., & Kuo, K. H. (2000). Materials Science and Engineering: A, 294, 242-245.
- Oleynikov, P. (2011). Cryst. Res. Technol. 46, No. 6, 569 – 579
- Rodrigues-Carvajal, J. (1998). Program FULLPROF-98, Version 0.2.
- Samuha, S., Grushko, B., & Meshi, L. (2016). J. Alloys Comp, 670, 18-24.
- Sugiyama, K., Saito, H., & Hiraga, K. (2002). J. Alloys Comp. 342, 148.
- Tasci, E.S., de la Flor, G., Orobengoa, D., Capillas, C., Perez-Mato, J.M., Aroyo, M.I.(2012). EPJ Web Conf. 22, 9.
- Uziel, A., Bram, A. I., Venkert, A., Kiv, A. E., Fuks, D., & Meshi, L. (2015). J. Alloys Comp, 648, 353-359.
- Yaniv, G., Fuks, D., & Meshi, L. (2018). Intermetallics, 100, 44-51.
- Yaniv, G., Vidal, D., Fuks, D., & Meshi, L. (2020). Metals, 10(4), 422.

Figure captions

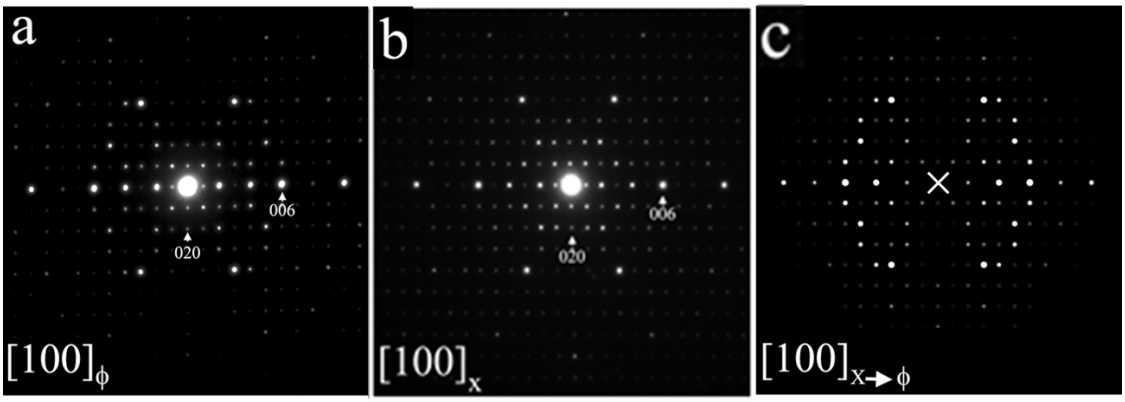

Figure 1 Experimental PED patterns along the [100] orientation of the: a) ϕ-phase, b) X-phase, and the corresponding PED pattern of the ϕ-phase (c) simulated by means of the eMAP software [Oleynikov, 2011]. For the simulations the structural model of the ϕ-phase was adopted from that of the X-phase where Re was replaced by Cr.

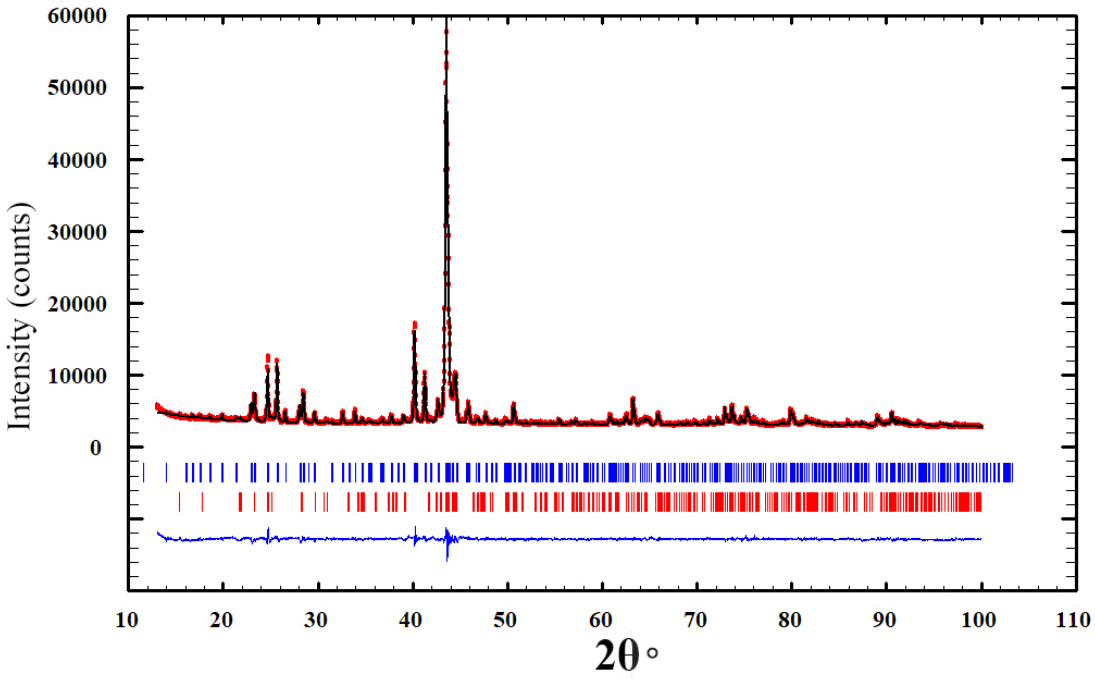

Figure 2 Plot of the Rietveld refinement of the powder XRD pattern of an $Al_{69.5}Cu_{20.0}Cr_{10.5}$ alloy showing the: observed XRD profile (red filled circles), calculated profile (black solid line) and difference between them (blue solid line). The vertical bars refer to the calculated peak positions of the ϕ-phase (upper blue bars) and Al_3Cu_4 (bottom red bars). (For the interpretation of the colors see the online version).

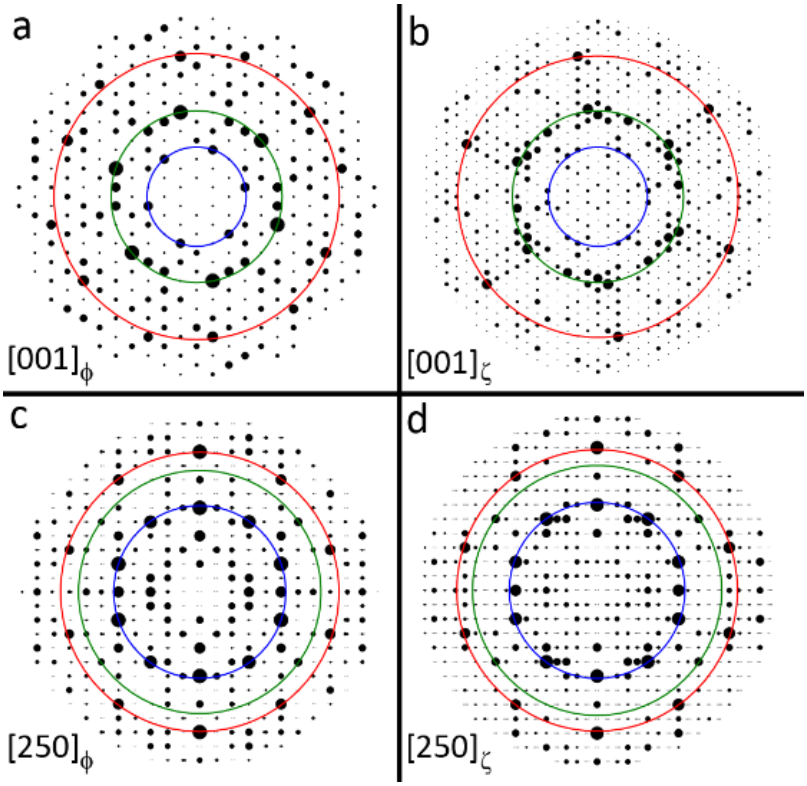

Figure 3 Simulated PED patterns along the [001] orientation and pseudo-10 fold [250] orientation of the ϕ-phase (a, c) and ζ-phase (b, d). (For interpretation of color in this figure legend, the reader is referred to the web version of this article).

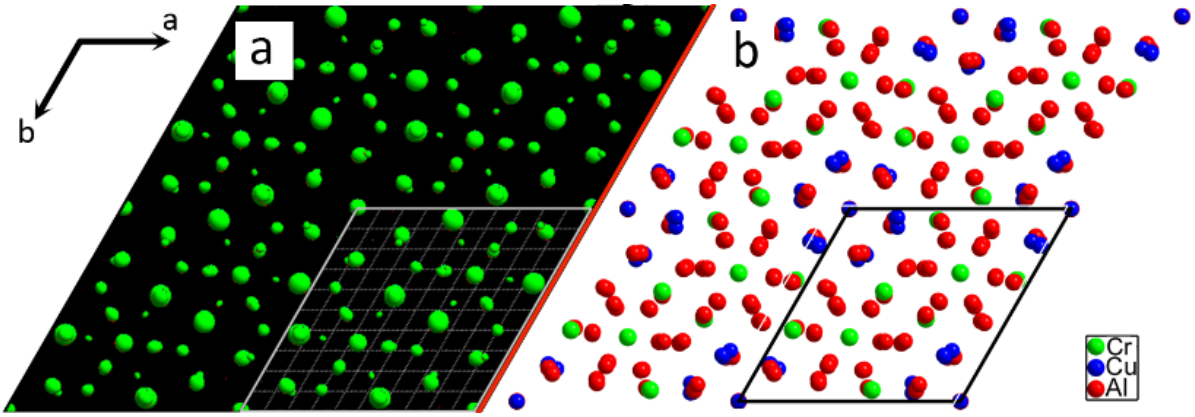

Figure 4 Deduced 3D electron density map of ϕ (a) and the structural model of ϕ determined experimentally (b) viewed along the [001] orientation. The Al, Cu and Cr type atoms are marked by red, blue and green, respectively. The map consists of the spherical maxima that represent the atom positions in the unit cell, and their magnitude can be related to the atom types. (For interpretation of color in this figure legend, the reader is referred to the web version of this article).

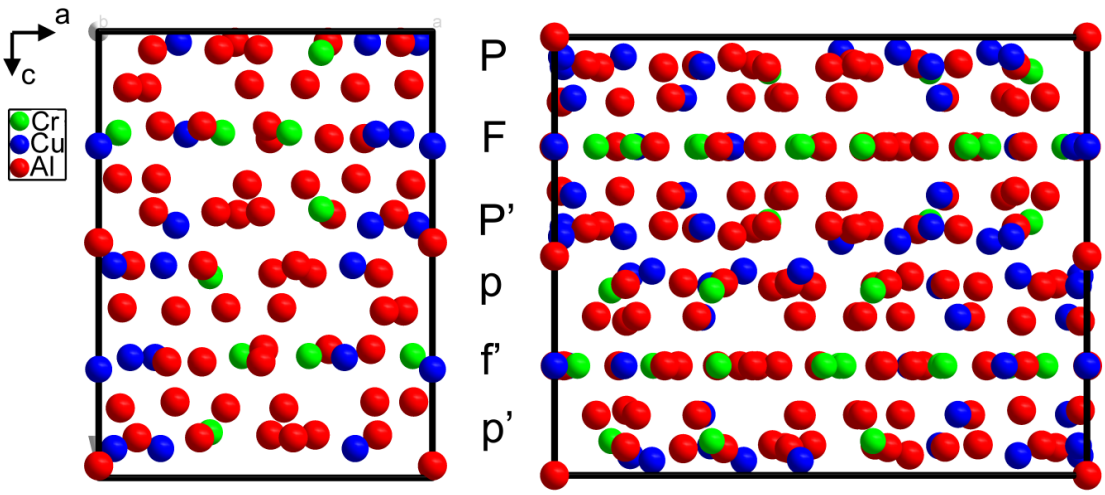

Figure 5 The structures of ϕ (left panel) and ζ (right panel) projected along the [010] orientation. (For interpretation of color in this figure legend, the reader is referred to the web version of this article).

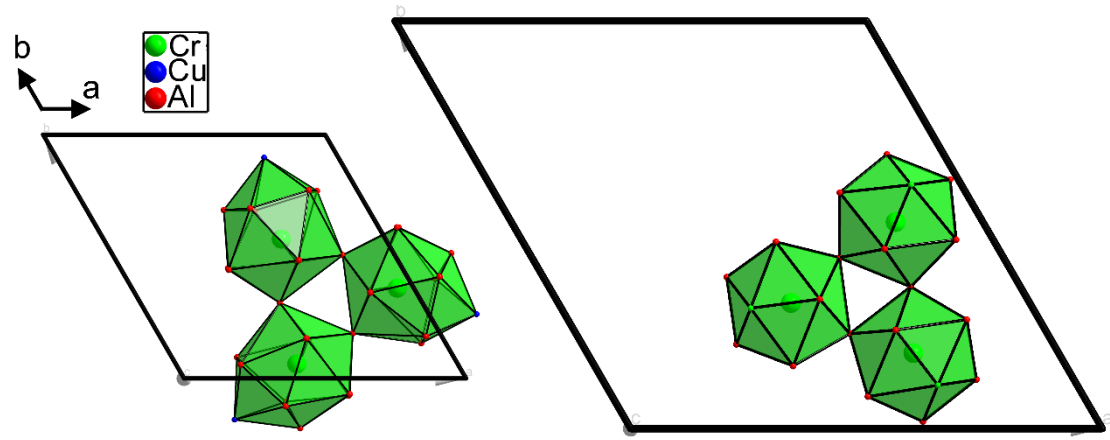

Figure 6 The I3-cluster in the structures of ϕ (left panel) and ζ (right panel) projected along the [010] orientation. (For interpretation of color in this figure legend, the reader is referred to the web version of this article).

Tables

Table 1 Details of the Rietveld refinement performed on the powder XRD data taken from the studied alloy.

Parameter	Data
Structure refined	ϕ-$Al_{69.2}Cu_{20.0}Cr_{10.8}$
Space group	$P6_3$
Unit cell parameter [nm]	a=1.0999(5) c=1.2697(9)
Additional phases generating diffraction peaks	ζ_{1Cu}-Al_3Cu_4 It was treated in the profile matching mode. Only the scale factors and lattice parameters were refined.
X-ray data range (2θ◦)	5.000-100.000

Zeroshift	0.00157
Peak profile	Pseudo-Voigt (η = 0.87452)
Half-width parameters	U = 0.011425, V = -0.005877, W = 0.016688
Asymmetry parameters	P_1 = 0.03012, P_2 = 0.04394
Total number of reflections (of ϕ phase)	524
Reliability factors	Rp = 2.66, Rwp = 3.49 , Rexp = 1.60, χ^2 = 4.77

Table 2 Atomic coordinates and thermal motion parameters for the ϕ-phase structure after the Rietveld refinement.

Name	Wyckoff site	x	y	z	B_{iso} [Å^2]	Occupancy
Cr1	6c	0.5682(2)	0.9391(3)	0.2718(0)	0.941	1
Cr2	2b	0.3333(3)	0.6666(7)	0.5875(1)	0.941	1
Cr3	2b	0.3333(3)	0.6666(7)	0.9357(7)	0.941	1
Cu1	6c	0.9547(5)	0.1964(6)	0.0564(8)	2.214	0.87
Al13	6c	0.9547(5)	0.1964(6)	0.0564(8)	0.159	0.13
Cu2	2a	0.0000(0)	0.0000(0)	0.2822(4)	2.214	1
Cu3	6c	0.9003(4)	0.1612(6)	0.2543(0)	2.214	0.86
Al12	6c	0.9003(4)	0.1612(6)	0.2543(0)	0.159	0.14
Cu4	6c	0.1943(4)	0.2396(1)	0.9618(2)	2.152	1
Al1	6c	0.6811(3)	0.0831(7)	0.0745(5)	0.159	1
Al2	6c	0.3815(1)	0.4581(5)	0.8754(0)	0.159	1
Al3	6c	0.7048(0)	0.2258(7)	0.2746(8)	0.159	1
Al4	6c	0.7675(9)	0.9291(7)	0.3640(3)	0.159	1
Al5	6c	0.3061(6)	0.8023(4)	0.2356(7)	0.159	1
Al6	6c	0.3578(3)	0.5249(3)	0.0700(1)	0.159	1
Al7	6c	0.4466(9)	0.0598(2)	0.1542(2)	0.159	1
Al8	6c	0.4838(8)	0.8468(6)	0.4356(7)	0.159	1
Al9	6c	0.1218(4)	0.4223(3)	0.9457(6)	0.159	1
Al10	6c	0.1448(8)	0.2390(5)	0.1566(1)	0.159	1
Al11	2a	0.0000(0)	0.0000(0)	0.9981(4)	0.159	1

Table 3 Interatomic distances for the ϕ-phase (in Å). CN is the coordination number. For simplicity, the coordination polyhedra of only heavy atoms are shown.

Cu4, CN=12			**Cu3|Al12, CN=13**			**Cu2, CN=13**		
1	Al4	2.4377	1	Cu2	2.5333	1	Al4	2.4952
1	Al1	2.4569	1	Cu1|Al13	2.5663	1	Al4	2.4959
1	Al11	2.4689	1	Al3	2.5942	1	Al4	2.4961
1	Al2	2.5040	1	Al4	2.6195	2	Cu3|Al12	2.5333
1	Al9	2.5138	1	Al7	2.6222	1	Cu3|Al12	2.5337

1	Al10	2.5324	1	Al10	2.684	1	Al11	2.7420
1	Cu3|Al12	2.6863	1	Cu4	2.6863	1	Al10	2.7941
1	Cu1|Al13	2.7137	1	Al10	2.7339	2	Al10	2.7944
1	Cu1|Al13	2.7206	1	Al2	2.7729	1	Cu4	3.3287
1	Al4	2.8776	1	Al4	2.9259	1	Cu4	3.3288
1	Al6	3.0539	1	Al1	3.1128	1	Cu4	3.3290
1	Cu2	3.3288	1	Al9	3.1655			
			1	Cr1	3.2308			

	Cu1|Al13, CN=11			**Cr3, CN=12**			**Cr2, CN=12**			**Cr1, CN=12**	
1	Al10	2.2874	1	Al6	2.4139	2	Al8	2.6658	1	Al8	2.2977
1	Al4	2.4678	1	Al6	2.4141	1	Al8	2.666	1	Al5	2.4454
1	Al7	2.5074	1	Al6	2.4145	1	Al3	2.7774	1	Al4	2.5363
1	Al11	2.5577	1	Al3	2.5007	1	Al3	2.7777	1	Al5	2.5387
1	Cu3|Al12	2.5663	1	Al3	2.5011	1	Al3	2.7778	1	Al2	2.705
1	Al1	2.6289	1	Al3	2.5012	1	Al1	2.8391	1	Al3	2.7328
1	Al9	2.6382	1	Al9	2.5297	2	Al1	2.8393	1	Al10	2.7467
1	Cu4	2.7139	2	Al9	2.5298	1	Al7	2.8882	1	Al7	2.7475
1	Cu4	2.7205	1	Al2	2.7096	1	Al7	2.8885	1	Al6	2.7897
1	Al8	3.0476	1	Al2	2.7099	1	Al7	2.8886	1	Al9	2.8462
1	Al10	3.0931	1	Al2	2.7105				1	Al1	2.8914
									1	Cu3/Al12	3.2311